Bias-dependent timing jitter of 1-GHz sinusoidally gated InGaAs/InP avalanche photodiode*

Ge Zhu(朱阁)[1], Fu Zheng(郑福)[2,3], Chao Wang(王超)[1,3], Zhibin Sun(孙志斌)[3], Guangjie Zhai(翟光杰)[3], and Qing Zhao(赵清)[1,†]

[1] School of Physics, Beijing Institute of Technology, Beijing 100081, China
[2] University of Chinese Academy of Sciences, Beijing 100049, China
[3] Key Laboratory of Electronics and Information Technology for Space Systems, National Space Science Center, Chinese Academy of Sciences, Beijing 100190, China

(Received 26 May 2016; revised manuscript received 7 July 2016; published online 30 September 2016)

We characterized the dependence of the timing jitter of an InGaAs/InP single-photon avalanche diode on the excess bias voltage (V_{ex}) when operated in 1-GHz sinusoidally gated mode. The single-photon avalanche diode was cooled to −30 degrees Celsius. When the V_{ex} is too low (0.2 V–0.8 V) or too high (3 V–4.2 V), the timing jitter is increased with the V_{ex}, particularly at high V_{ex}. While at middle V_{ex} (1 V–2.8 V), the timing jitter is reduced. Measurements of the timing jitter of the same avalanche diode with pulsed gating show that this effect is likely related to the increase of both the amplitude of the V_{ex} and the width of the gate-on time. For the 1-GHz sinusoidally gated detector, the best jitter of 93 ps is achieved with a photon detection efficiency of 21.4% and a dark count rate of $\sim 2.08\times10^{-5}$ per gate at the V_{ex} of 2.8 V. To evaluate the whole performance of the detector, we calculated the noise equivalent power (NEP) and the afterpulse probability (P_{ap}). It is found that both NEP and P_{ap} increase quickly when the V_{ex} is above 2.8 V. At 2.8-V V_{ex}, the NEP and P_{ap} are $\sim 2.06\times10^{-16}$ W/Hz$^{1/2}$ and 7.11%, respectively. Therefore, the detector should be operated with V_{ex} of 2.8 V to exploit the fast time response, low NEP and low P_{ap}.

Keywords: timing jitter, avalanche photodiode, excess bias voltage, single-photon detector

PACS: 85.60.Bt, 85.60.Gz **DOI:** 10.1088/1674-1056/25/11/118505

1. Introduction

Single-photon detectors are essential components for many applications, such as quantum communication,[1–4] laser ranging,[5–9] circuit testing,[10] and optical time-domain reflectometer (OTDR).[11] Recently, quantum key distribution (QKD) of the long transmission distance and high key generation rate draw intense research on high-speed, near-infrared single-photon detectors.[12–15] Two main candidates are superconducting nanowire single-photon detectors (SSPDs) and InGaAs/InP single-photon avalanche photodiodes (SPADs). SSPDs provide outstanding performance in low dark count rate, high detection efficiency, and low timing jitter, especially in the near-infrared wavelength. In spite of these preferable advantages, SSPDs have drawbacks for many practical applications: requirement of cryogenic temperatures (< 4 K) to keep the superconducting state.[15] Refrigeration systems to maintain cryogenic conditions are very large and have high energy consumption. In contrast, InGaAs/InP avalanche photodiodes (APD) based SPADs are compact, energy saving and low cost, and they also provide high performance in the near-infrared spectrum. Therefore, InGaAs/InP-based SPADs are widely used in many applications, especially in the QKD systems.[12–14]

Unfortunately, InGaAs/InP-based SPADs also suffer from significant dark counts when operated in the geiger-mode. To reduce the dark counts, the gated mode operation is widely employed.[16] However, in the gated mode, the weak avalanche signals are usually buried in the gating noise due to the charge–discharge response of APD capacitance to the gating signal. To discriminate the avalanche signals, the gating noise should be removed when possible. Recently, some novel gating techniques have been reported to suppress the gating noise while increasing the gating signal repetition rate over 1 GHz.[17–19] One approach is sinusoidal gating. Due to the frequency response of the sinusoidal gating signal to the APD capacitance is distributed at the frequency of the gating signal and its harmonic frequencies; therefore, the fundamental component and the higher harmonics can be easily removed by narrow band elimination filters (BEFs) and low pass filters (LPFs), respectively. On the other hand, the energy of the avalanche signal contains many frequency components and almost all of them can pass through the BEF.[17] In order to improve the performance, several sinusoidal gating techniques have been demonstrated. In Ref. [20], two balanced APDs are used to make the gating frequency tunable. By using the sinusoidal harmonic subtraction method, single-photon detection

*Project supported by the National Natural Science Foundation of China (Grant Nos. 11275024, 61274024, and 61474123), the Youth Innovation Promotion Association, China (Grant No. 2013105), and the Ministry of Science and Technology of China (Grant Nos. 2013YQ030595-3 and 2011AA120101).

†Corresponding author. E-mail: qzhaoyuping@bit.edu.cn

© 2016 Chinese Physical Society and IOP Publishing Ltd

efficiency up to 50% at 1310 nm has been achieved.[21] In the typical sinusoidal gating scheme, the BEF causes some distortion to the avalanche signals and results in a relatively large timing jitter for single-photon detection,[17,22] limiting its applications in high speed QKD or ultra-sensitive laser ranging. To circumvent the problem on the BEF, reference [22] uses a low pass filtering (LPF) technique to minimize the distortion to the avalanche signals and realize a 1-GHz sinusoidal gating detector with a timing jitter as low as 60 ps. In Ref. [23], the timing response of a sinusoidally gated InGaAs/InP APD both in synchronous mode and free-running mode has been investigated at a fixed V_{ex}. However, the timing response of a single-photon detector is a strong function of detector bias conditions.[24,25] Moreover, for sinusoidal gating, when the excess bias voltage (V_{ex}) is increased by increasing the direct-current (DC) bias voltage with fixed sine wave voltage, the applied gate-on time (T_g) is also increased. This may increase the timing jitter, especially in the high speed sinusoidal gating scheme, where the optical response of the avalanche photodiode is comparable with the T_g.[16]

In this paper, we concentrate on the comprehensive characterization of the bias-dependent timing jitter of a 1-GHz sinusoidally gated InGaAs/InP APD. In our measurements, the APD was cooled to −30 degrees Celsius and the threshold voltage for the avalanche discrimination was set to −33 mV. Under middle V_{ex} conditions, an increase in the V_{ex} reduces the jitter; however, at low and high V_{ex}, we show that increasing the V_{ex} also has the effect of increasing the jitter. The smallest jitter of 93 ps is obtained at 2.8-V V_{ex}. In addition, the photon detection efficiency and the dark count rate of the detector are 21.4% and $\sim 2.08\times10^{-5}$ per gate, respectively. The timing jitter measurement of the same APD but using pulse gating shows that this effect is likely related to the increment of the T_g when the V_{ex} is increased. Finally, we calculate the noise equivalent power (NEP) and the afterpulse probability (P_{ap}) of the detector, and find that both of them rise quickly at V_{ex} that exceed 2.8 V. We may conclude that the detector should be operated at V_{ex} of 2.8 V to exploit the fast time response (93 ps), low NEP ($\sim 2.06\times10^{-16}$ W/Hz$^{1/2}$) and low P_{ap} (7.11%).

2. Experimental setup

Figure 1(a) shows the experimental setup for studying the bias-dependent timing jitter of a sinusoidally gated InGaAs/InP avalanche photodiode. The Fiber–Pigtailed InGaAs/InP APD (PGA-400, Princeton Lightwave Inc.) was cooled to −30 degrees Celsius. The sine wave signal at a frequency of 1 GHz was produced by a standard signal generator (MG645B) and amplified by a high power amplifier (H-Amp, Mini-circuits, ZHL-42W). Through a coupler, 90% of the signal was passed through a band pass filter (BPF) to provide the gating signal with a peak-to-peak amplitude of $6V_{p-p}$, which was combined with the DC reverse bias voltage (V_{DC}) and supplied to the APD by using the gated passive quenching circuit (GPQC).[17] Here, the BPF was used to eliminate the amplified sideband noise and harmonic noise. The other 10% was used to trigger the pulse laser. The trigger rate for the laser was set to 20 MHz by a prescaler whose divide ratio was 50. The pulsed diode laser (PDL 800-B, PicoQuant) emitted 30-ps laser pulses at 1550 nm wavelength. They were attenuated to 0.1 average photons per pulse by an optical attenuator (ATT, FVA-3150 EXFO) and coupled into the APD by single-mode fibers. In order to obtain the maximum photon detection efficiency (PDE), a delay module was used to tune the phase between the photon signal arrival and the gating signal. The output signals from the APD were processed by a band elimination filter (BEF), a low pass filter (LPF) and another two low noise amplifiers (LN-Amp, Mini-circuits, ZFL-1000LN+) to extract the avalanche signals. The BEF suppressed the capacitance response of the APD to the gating signal at the fundamental frequency of 1-GHz. Then the signals were amplified

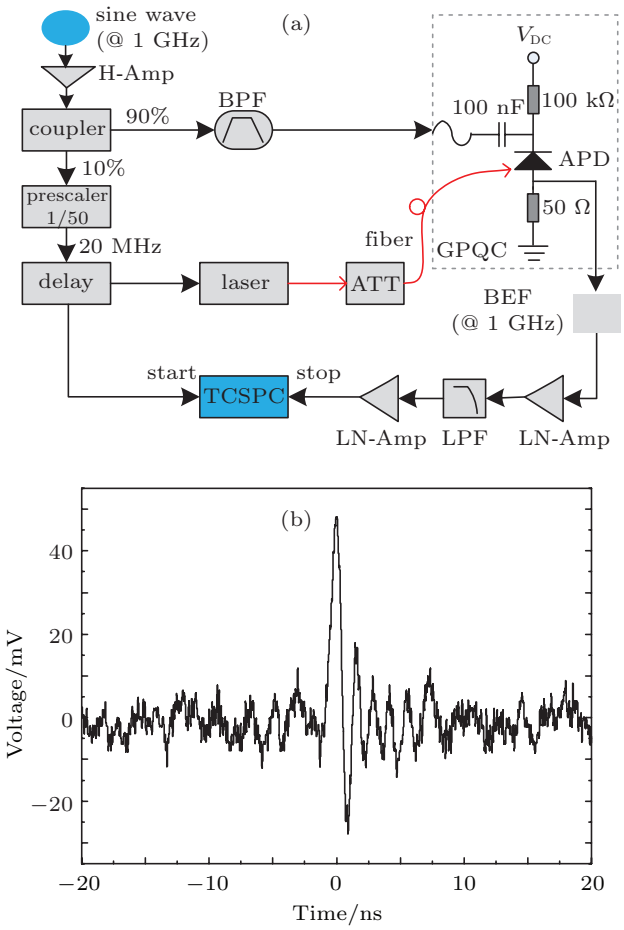


Fig. 1. (color online) (a) Schematic diagram of the experimental setup for studying the bias-dependent timing jitter of a sinusoidally gated InGaAs/InP avalanche photodiode. H-Amp: high power amplifier; BPF: band pass filter; GPQC: gated passive quenching circuit; BEF: band elimination filter; LN-Amp: low noise amplifier; LPF: low pass filter; ATT: optical attenuator; TCSPC: time-correlated single-photon counting module. (b) Oscilloscope trace of the extracted avalanche signal after the second LN-Amp.

by a LN-Amp with a gain of 23 dB and subsequently led to a low pass filter (LPF) with a cutoff frequency of 1.5 GHz, which was used to reject the higher harmonics generated by a nonlinear capacitance response of the APD. Consequently, the noise level after the LPF was close to the thermal noise limit and the avalanche signals were distilled well. Before entering the time-correlated single-photon counting module, the avalanche signals were further amplified by another LN-Amp. Figure 1(b) shows a typical avalanche signal amplified by the second LN-Amp.

Photon arrivals are discriminated by sensing the leading edge of the avalanche current with a suitable threshold. Due to finite carrier propagation velocities and spatially different fields within the volume of the APD, the time from photon absorption to discrimination of avalanche current is not a fixed delay. This causes the timing jitter of the detector.[25] To characterize bias-dependent timing jitter of the 1-GHz sinusoidally gated InGaAs/InP APD detector we used a TCSPC technique, whereby a histogram representing the probability distribution of time delays from the arrival of photons to the detection of the corresponding avalanche signals was accumulated. The timing jitter is usually defined as the full width of the maximum (FWHM) of the histogram. As shown in Fig. 1(a), a standard TCSPC module (SPC 130, Becker & Hickl GmbH) was used. The "Start" port of the TCSPC module was synchronized with the laser triggering signal, while the "Stop" port was triggered by the amplified avalanche signals. All the measurements reported in this paper were taken when the TCSPC module was configured with a time resolution of 8 ps (FWHM).

3. Bias-dependent timing jitter performance and analysis

Since timing jitter is a strong function of detector bias voltage conditions, detector temperature, as well as the spatial position of the photon absorption in the detector, as has been observed in a silicon Geiger mode single-photon detector.[24] Therefore, we fixed the temperature of the detector to −30 degrees Celsius and investigated the timing response only by changing the applied DC bias voltage. On the other hand, the timing jitter improves by reducing the threshold voltage of the timing discriminator of the TCSPC module.[26,27] In our measurements, the threshold voltage was set to −33 mV. Because the avalanche signals were inverted before leading to the timing discriminator. Figure 2(a) presents the timing jitter as a function of the excess bias voltage (V_{ex}). As shown in the inset of Fig. 2(a), the V_{ex} is the voltage that exceeds the avalanche breakdown voltage (V_B) of the APD and adjusted by changing the V_{DC} from 0.2 V to 4.2 V in 0.2-V step. From Fig. 2(a) we can see that the timing jitter of the detector firstly increases at low V_{ex} (0.2 V–0.8 V). Then the timing jitter decreases with further increasing V_{ex} (1 V–2.8 V). Finally, the timing jitter increases again at high V_{ex} (3 V–4.2 V). The best jitter of 93 ps was achieved with a detection efficiency of 21.4% at the V_{ex} of 2.8 V. Figure 2(b) shows a typical normalized timing jitter histogram recorded by the TCSPC module at an excess bias of 2.8 V, corresponding to a PDE of 21.4%. From the histogram a timing jitter of 93 ps (FWHM) can be determined.

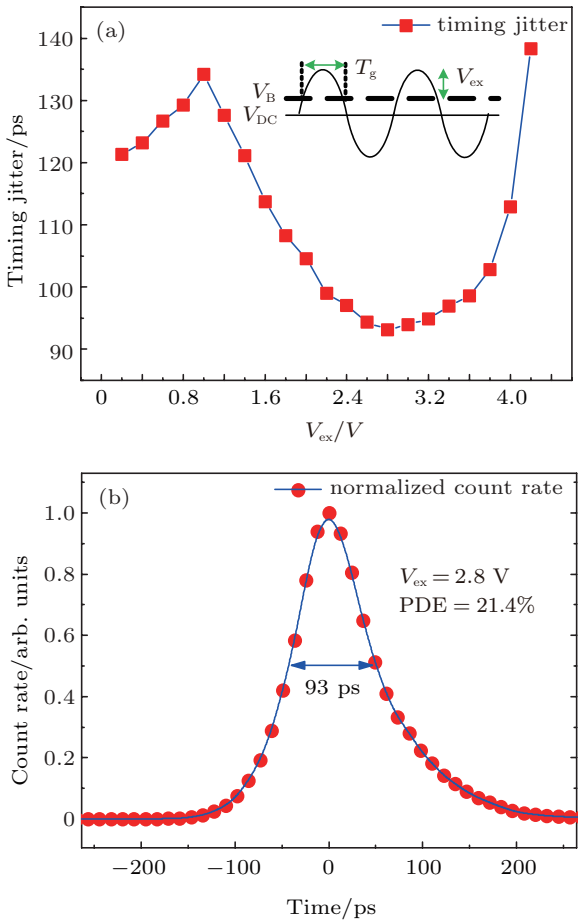


Fig. 2. (color online) (a) Bias-dependent timing jitter of the 1-GHz sinusoidally gated InGaAs/InP APD single-photon detector. (b) Normalized instrumental response of the system with 93 ps (FWHM) at the V_{ex} of 2.8 V, and the PDE is 21.4%.

It has been reported that the timing jitter decreases with increasing avalanche mean propagation speed.[24] The mean propagation speed of the avalanche is given by

$$V_p = CI_f, \tag{1}$$

where V_p represents the mean propagation speed of the avalanche, C is a constant, and I_f is the final avalanche current. Equation (1) indicates that V_p is proportional to the I_f, given by

$$I_f = (V - V_B)/R_d, \tag{2}$$

where V and V_B are the applied bias voltage and the avalanche breakdown voltage, respectively, and R_d is the diode series resistance. Here, $(V - V_B)$ is called the excess bias voltage V_{ex}. In addition, V_B and R_d are constants at a fixed temperature. As

a result, the timing jitter is dependent on the V_{ex}. However, for the high speed sinusoidally gated scheme, the V_{ex} is not as flat as in the pulse gating scheme. When the V_{ex} is increased by increasing the V_{DC}, the gate-on time (T_g) also increases as illustrated in the inset of Fig. 2(a). On the other hand, in the 1-GHz sinusoidal gating scheme, the T_g only has several hundred picoseconds which is comparable with the single-photon optical response time.[23] Thus, wider T_g is likely to cause larger timing jitter. Therefore, the evaluation of timing jitter performance of the high speed sinusoidally gated single-photon detector should take into account both V_{ex} and T_g. In Fig. 2(a), at low V_{ex} (0.2 V–0.8 V), the timing jitter increases with V_{ex}. This indicates that at low V_{ex} the main contribution to the timing jitter is given by the increased T_g, which makes a wider distribution of the single-photon optical response time within T_g. However, with the V_{ex} increasing further (1 V–2.8 V), the timing jitter reduces, because under this condition the increased V_{ex} plays a dominant role and the V_p of the avalanche is increased with V_{ex}, leading to smaller timing jitter.[24] At higher V_{ex} (3 V–4.2 V), the V_p maybe get saturated, then the T_g plays a dominant role and the timing jitter increases again with the V_{ex}.

To verify our explanation for the timing jitter performance in the 1-GHz sinusoidal gating scheme, we performed the similar timing jitter measurements on the same InGaAs/InP APD except that the 1-GHz sinusoidal gating was replaced by the 20-MHz pulse gating. The pulse gating with an amplitude of 3 V was generated by a function generator (AFG3022C) and the T_g was set to 16 ns, 20 ns, and 24 ns, respectively. In order to extract the weak avalanche signals buried in the gating spike noise, we used the self-differencing technique which is based on subtracting the output signal of the APD from a replica delayed by exactly one gate period.[18] In our experiment, the APD output was divided into two equal components with a 50/50 power spliter (Mini-circuits, ZAPD-2-252-S+), which were then subtracted by a power combiner (Mini-circuits, ZFSCJ-2-1-S+). The coaxial cables connecting the spliter and the combiner have different lengths to induce a delay of one gate period (50 ns). Thus, the avalanche signals can be obtained at the output of the power combiner. The avalanche signals were then amplified and sent to the TCSPC module. Compared to the sinusoidal gating, the T_g in the pulse gating is invariable when the V_{ex} is increased, as shown in the inset of Fig. 3. The dependence of the timing jitter of the pulse gated detector on the V_{ex} is shown in Fig. 3. As has been demonstrated in previous research, the jitter reduces with increasing V_{ex}.[21,23,24] Moreover, at low V_{ex}, the jitter reduces quickly, while at high V_{ex} the decrement reduces, maybe due to a saturation effect in V_p. On the other hand, for the same V_{ex}, the longer the gate-on time, the larger the timing jitter. In addition, compared to the timing jitter in the 1-GHz sinusoidal gating detector, the jitter in the pulse gating scheme significantly increases. These results manifestly demonstrate that a wider gate-on time is likely to result in a larger timing jitter.

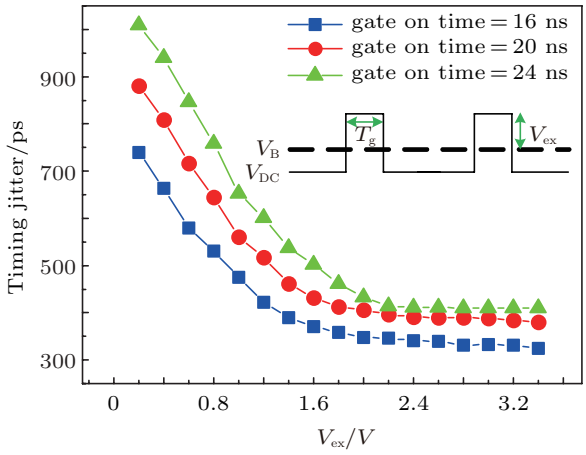


Fig. 3. (color online) Bias-dependent timing jitter of the 20-MHz pulse gated single-photon detector with the same InGaAs/InP APD when the gate-on time is 16 ns, 20 ns, and 24 ns, respectively.

4. Discussion

To evaluate the whole performance of the 1-GHz sinusoidal gating detector, it is necessary to introduce the noise equivalent power (NEP). The NEP is a useful figure of merit for photon-counting detectors because it incorporates both detection efficiency and dark count probability. The equation used to calculate the NEP is given by[28]

$$\mathrm{NEP} = \frac{h\nu}{\mathrm{PDE}}\sqrt{2\mathrm{DCR}}, \tag{3}$$

where h is Planck's constant, ν is the frequency of the photons, PDE is the photon detection efficiency, and DCR is the dark count rate integrated over one second. The PDE is calculated by[29]

$$\mathrm{PDE} = \frac{1}{\mu}\ln\left(\frac{1-P_{dc}}{1-P_{de}}\right), \tag{4}$$

where μ is the mean photon number per laser pulse, P_{dc} is the dark count probability per gate, and P_{de} is the photon detection probability per laser pulse. Figure 4(a) shows the performance of the detector in terms of PDE and DCR. According to the detection efficiency and dark count rate, the NEP versus V_{ex} is calculated, as shown in Fig. 4(b). The dashed line in Fig. 4(b) indicates that the NEP is relatively constant at low V_{ex}, from 0.2 V to 2.8 V and at 2.8 V V_{ex} the NEP and the dark count rate are $\sim 2.06\times10^{-16}$ W/Hz$^{1/2}$ and $\sim 2.08\times10^{-5}$ per gate, respectively; however, the smallest timing jitter of 93 ps is achieved at V_{ex} of 2.8 V (see Fig. 4). On the other hand, both the NEP and the timing jitter increase at high V_{ex}, from 3 V to 4.2 V. In addition, for the high-speed InGaAs/InP APD based single-photon detector, the afterpulse probability is quite an important factor for the performance of the detector. The afterpulse

probability P_{ap}, defined here as the ratio of the total afterpulse counts to the photon counts, can be obtained from[18]

$$P_{ap} = \frac{(R_{NI} - R_D)(f_g/f_L)}{R_I - R_{NI}}, \quad (5)$$

where R_I and R_{NI} meant the count rate per gate in the illuminated gate and non-illuminated gate respectively, while R_D was the dark count rate, when the laser was closed. Here, f_g and f_L referred to the frequency of sinusoidal gating (1 GHz) and the laser pulse repetition rate (20 MHz) respectively. In the measurement, the dead time of the TCSPC was 100 ns. An inset was provided in Fig. 4(b) to illustrate the P_{ap} performance at different V_{ex}. At 2.8-V V_{ex} the P_{ap} is 7.11%, while when the V_{ex} exceeds 2.8 V, it increases quickly. Therefore, for use in photon-counting applications, it would be beneficial to operate this detector at 2.8 V excess bias to exploit the fast time response, the low NEP as well as the low P_{ap}.

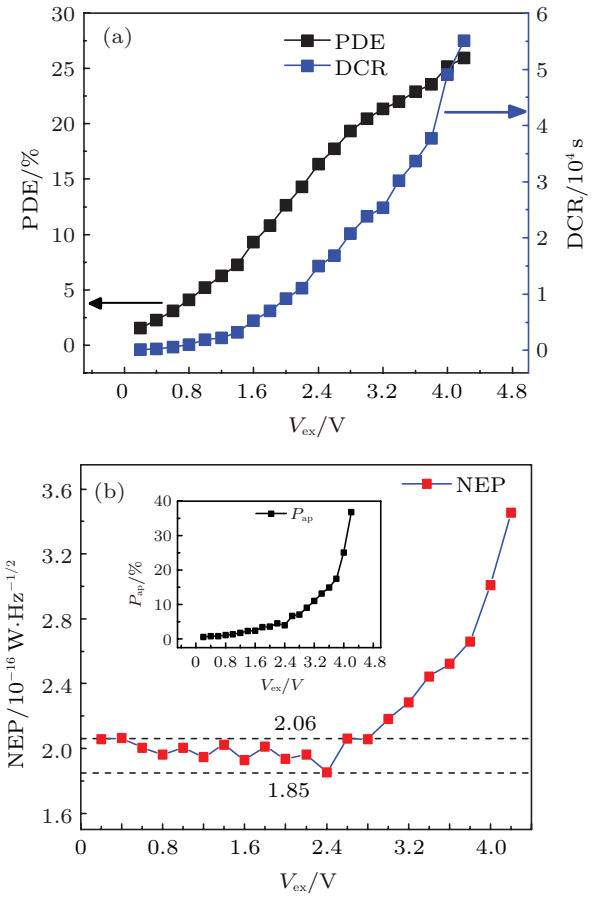


Fig. 4. (color online) (a) Photon detection efficiency and dark count rate as a function of excess bias voltage. (b) Noise equivalent power versus excess bias voltage. The dashed horizontal lines denote the range of noise equivalent power at low V_{ex}. The inset graph shows the P_{ap} performance with the increased V_{ex}.

5. Conclusion

In this paper, we report on the dependence of the timing jitter on the excess bias voltage (V_{ex}) of 1-GHz sinusoidally gated InGaAs/InP APD single-photon detector. It is found that the jitter increases at low and high V_{ex}, while it decreases at middle V_{ex}. By taking further timing jitter measurement of the same InGaAs/InP APD with pulsed gating, we conclude that this effect is likely related to the increase of both the V_{ex} amplitude and the width of the gate-on time (T_g).

According to our explanation, at low (0.2 V–0.8 V) and high (3 V–4.2 V) V_{ex}, the main contribution to the increase of the timing jitter is the increasing width of the T_g. While at middle V_{ex} (1 V–2.8 V), the increasing of the V_{ex} plays a dominant role in reducing the timing jitter by accelerating the avalanche buildup. The best timing jitter of 93 ps is achieved at the V_{ex} of 2.8 V. Under this condition, the dark count rate is $\sim 2.08\times10^{-5}$ per gate and the photon detection efficiency is 21.4%. We also calculate the noise equivalent power (NEP) and the afterpulse probability (P_{ap}). The results indicate that the NEP is relatively constant at small V_{ex} that is less than 2.8 V, while it quickly rises when the V_{ex} is increased above 3 V. A NEP of $\sim 2.06\times10^{-16}$ W/Hz$^{1/2}$ is achieved at 2.8-V V_{ex}. Coincidentally, the P_{ap} is also increased quickly when the V_{ex} is beyond 2.8 V. At 2.8-V V_{ex}, the P_{ap} is 7.11%. Therefore, it would be beneficial to operate this detector at an excess bias of 2.8 V to exploit the fast time response, low NEP and low P_{ap}. They are 93 ps, $\sim 2.06\times10^{-16}$ W/Hz$^{1/2}$ and 7.11%, respectively. Besides, the photon detection efficiency is 21.4% with the dark count rate of $\sim 2.08\times10^{-5}$ per gate.

References

[1] Hadfield R H 2009 *Nat. Photon.* **3** 696
[2] Zhang J, Itzler M A, Zbinden H and Pan J W 2015 *Light Sci. Appl.* **4** e286
[3] Quan D X, Zhu C H, Liu S Q and Pei C X 2015 *Chin. Phys. B* **24** 050309
[4] Jiao R Z, Feng C X and Ma H Q 2008 *Acta. Phys. Sin.* **57** 1352 (in Chinese)
[5] McCarthy A, Krichel N J, Gemmell N R, Ren X, Tanner M G, Dorenbos S N, Zwiller V, Hadfield R H and Buller G S 2013 *Opt. Express* **21** 8904
[6] Chen S J, Liu D K, Zhang W X, You L X, He Y H, Zhang W J, Yang X Y, Wu G, Ren M, Zeng H P, Wang Z, Xie X M and Jiang M H 2013 *Appl. Opt.* **52** 3241
[7] Zhou H, He Y H, You L X, Chen S J, Zhang W J, Wu J J, Wang Z and Xie X M 2015 *Opt. Express* **23** 14603
[8] Ren M, Gu X R, Liang Y, Kong W B, Wu E, Wu G and Zeng H P 2011 *Opt. Express* **19** 13497
[9] Liang Y, Huang J H, Ren M, Feng B C, Chen X L, Wu E, Wu G and Zeng H P 2014 *Opt. Express* **22** 4662
[10] Stellari F, Tosi A, Zappa F and Cova S 2004 *IEEE Trans. Instrum. Meas.* **53** 163
[11] Levine B F, Bethea C G and Campbell J C 1984 *Electron. Lett.* **20** 596
[12] Namekata N, Takesue H, Honjo T, Tokura Y and Inoue S 2011 *Opt. Express* **19** 10632
[13] Zhang J, Eraerds P, Walenta N, Barreiro C, Thew R and Zbinden H 2010 *Proc. SPIE* 76810Z-1
[14] Dixon A R, Yuan Z L, Dynes J F, Sharpe A W and Shields A J 2008 *Opt. Express* **16** 18790
[15] Natarajan C M, Tanner M G and Hadfield R H 2012 *Supercond. Sci. Technol.* **25** 063001
[16] Ribordy G, Gisin N, Guinnard O, Stuck D, Wegmuller M and Zbinden H 2004 *J. Mod. Opt.* **51** 1381
[17] Namekata N, Adachi S and Inoue S 2009 *Opt. Express* **17** 6275
[18] Yuan Z L, Kardynal B E, Sharpe A W and Shields A J 2007 *Appl. Phys. Lett.* **91** 041114

[19] Zhang J, Thew R, Barreiro C and Zbinden H 2009 *Appl. Phys. Lett.* **95** 091103
[20] Campbell J C, Sun W L, Lu Z W, Itzler M A and Jiang X D 2012 *IEEE J. Quant. Electron.* **48** 1505
[21] Restelli A, Bienfang J C and Migdall A L 2013 *Appl. Phys. Lett.* **102** 141104-1
[22] Liang Y, Wu E, Chen X L, Ren M, Jian Y, Wu G and Zeng H P 2011 *IEEE Photon. Technol. Lett.* **23** 887
[23] Ren M, Liang Y, Sun W L, Wu G, Campbell J C and Zeng H P 2014 *IEEE Photon. Technol. Lett.* **26** 1762
[24] Lacaita A, Mastrapasqua M, Ghioni M and Vanoli S 1990 *Appl. Phys. Lett.* **57** 489
[25] Farr W H and Birnbaum K 2010 *Proc. SPIE* 76810U-1
[26] Gulinatti A, Maccagnani P, Rech I, Ghioni M and Cova S 2005 *Electron. Lett.* **41** 272
[27] Ingargiola A, Assanelli M, Gallivanoni A, Rech I, Ghioni M and Cova S 2009 *Proc. SPIE* 73200K-1
[28] Sun Z B, Ma H Q, Lei M, Yang H D, Wu L A, Zhai G J and Feng J 2007 *Acta. Phys. Sin.* **56** 5790 (in Chinese)
[29] Zheng F, Wang C, Sun Z B and Zhai G J 2016 *Chin. Phys. B* **25** 010306